J. Anat. (1989), **163**, pp. 261–273
With 9 figures
Printed in Great Britain

Specific heart granules and natriuretic peptide in the developing myocardium of fetal and neonatal rats and hamsters

V. NAVARATNAM, J. M. WOODWARD AND J. N. SKEPPER

Department of Anatomy, University of Cambridge, Downing Street, Cambridge CB2 3DY, England

(*Accepted* 10 *August* 1988)

INTRODUCTION

Over the past decade much has been learned regarding the content and possible functional implications of specific heart granules (SHG). The injection of granule-rich fractions induces natriuresis and diuresis (De Bold, Borenstein, Veress & Sonnenberg, 1981) and a family of polypeptides, which are now generically known as atrial natriuretic peptides (ANP), has been isolated and sequenced (Currie *et al.* 1984); the physiological evidence suggests that the release of active components of these granule-stored peptide hormones could play a substantial role in the control of extracellular fluid volume by invoking mechanisms such as natriuresis and diuresis as well as vasodilatation and diminution of cardiac output (Cantin & Genest, 1985). The literature contains descriptions of A and B granule sub-populations but there is no evidence that they differ in peptide content and, indeed, detailed ultrastructural analysis has shown that the differences in appearance are caused by varying sectional planes (Skepper & Navaratnam, 1988).

Some information is also available in the literature on the ontogenesis of SHG and ANP during fetal and neonatal life. Although SHG are predominantly restricted to atrial muscle in adult mammals, they are initially developed in both atria and ventricles during fetal life (see Challice & Virágh, 1973), a distribution which is retained in adult animals of lower vertebrate classes (Bencosme & Berger, 1971; Yunge *et al.* 1980). Moreover, radioimmunoassay findings on the cord blood of human neonates indicate that ANP may be present in higher concentrations than in the adult circulation (Tulassay, Rascher & Lang, 1986) supporting the view that ANP activity may be more pronounced at late fetal and neonatal stages. In a previous study on fetal development in the rat (Pager, 1968), electron-dense granules similar to SHG were observed in atrial and ventricular myocytes from the fourteenth day of gestation and Dolan & Dobroszi (1986), using radioimmunoassay of pooled atria, found measurable quantities of ANP at a similar stage. However, in a recent study on rat fetuses, relying largely on light microscopic techniques for antigen detection, Toshimori, Toshimori, Oura & Matsuo (1987*a*) have described weak ANP-like immunoreactivity as early as the eleventh day of gestation which, if confirmed, suggests that the earliest appearance of ANP is more or less concurrent with that of myofibrils.

The present investigation was conducted to determine the pattern of onset and development of ANP synthesis and storage in the rat heart using transmission electron microscopy, immunocytochemistry and radioimmunoassay for ANP-28. The sequence of development in the rat is compared with that in the hamster, a species in which the

density of SHG in cardiac myocytes and the corresponding level of atrial ANP immunoreactivity are lower (Navaratnam, 1987), although the levels of plasma immunoreactivity are similar.

MATERIALS AND METHODS

The material used in this study included hearts from rat fetuses (10, 11, 12, 13, 14, 15, 18 and 20 days gestation, the morning of finding a vaginal plug being designated the first day), rat neonates (2, 5, 15 days and 6 weeks after birth) and young adult rats (6 months) as well as hearts from hamster fetuses (10, 11, 12, 14 and 16 days), hamster neonates (2, 5, 10 and 15 days) and 6 months old hamsters. Fetuses and neonates were killed by decapitation while adults were killed by a blow to the head without anaesthetic.

Immunocytochemistry

The hearts were perfused through the left ventricle with Pipes buffer and saline perfusate at pH 7·4 followed by perfusion fixation with a solution containing 2% formaldehyde and 2% glutaraldehyde in Pipes buffer at 20 °C and pH 7·2. Early fetal hearts too small for perfusion were fixed by immersion in similar fluid. The hearts were then removed and some material was embedded in Taab resin after secondary fixation in 1% osmium tetroxide, bulk staining in uranyl acetate and dehydration using a graded ethanol series. The remaining samples were partially dehydrated in the unosmicated state to 75% ethanol and they were embedded in LR white by infiltration and polymerisation *in vacuo* at 47 °C. Thin sections (40–60 nm) were cut on a Huxley Mk I ultramicrotome, mounted on nickel or copper grids and left overnight to dry.

Sections from LR white-embedded specimens were processed for antigen detection as follows: non-specific labelling was blocked by floating grids face down on a drop of tris buffered saline (TBS) at pH 7·6 containing 2% bovine serum albumin (BSA), 0·2% Tween 20, 0·1% Triton X-100 and 0·0001% Thimerosal for 1·5 hours. The grids were then floated for 16 hours in a moist chamber face down on drops of primary antiserum (Peninsula Laboratories anti-rat ANP-28 serum raised in rabbits; 100% cross-reactive with the equivalent human peptide and cross-reactive with the hamster peptide as evinced by radioimmunoassay and immunogold preparations), diluted 1:500 in the blocking solution. Sections were washed in TBS containing 0·1% BSA, 0·2% Tween 20 and 0·1% Triton X-100 for 1 hour and then floated for 1 hour on drops of colloidal gold-labelled goat anti-rabbit secondary antibodies (15 nm particles) diluted in TBS. After washing with TBS and double distilled water, the sections were finally stained in uranyl acetate and lead tartrate (45 seconds in each).

Sections of tissues embedded in Taab resin were immunolabelled by preceding the procedure described above with etching in 4% aqueous sodium metaperiodate for 1 hour; the antiserum was diluted 1:50. Immunocytochemical controls were conducted either by the omission of primary antiserum or by pre-incubation of primary antiserum with ANP-28. The sections were viewed and photographed in a Philips EM 300.

Semithin sections of LR white-embedded material were immunolabelled and viewed under the light microscope after silver intensification using Janssen's Intense-II kit (Danscher & Rytter Nörgaard, 1985).

Radioimmunoassay

For RIA at least two litters and six samples from each stage were used though, for the youngest fetuses possessing very tiny heart rudiments, a minimum of 4 hearts per

tube sample was used. In the postnatal material and in fetal hearts where the relevant chambers could be distinguished, tissue was taken from the left and right auricular appendages and from the costal surface of the left ventricle just above the apex. The tissue was washed in saline to remove excess blood, blotted dry and weighed. The fragments were rapidly transferred to boiling acetic acid (0·1 M) and left for 15 minutes to abolish any endogenous proteolytic activity. The tissue was subsequently sonicated in a MSE Sonitron 150 and centrifuged in a bench microfuge after which the supernatant was removed with additional cold 0·1 M acetic acid. The extract was then rapidly frozen and stored at −70 °C until assay. In immature fetuses where cardiac chambers could not be distinguished, the entire heart rudiment was removed and processed.

The extracts were dried at 40 °C *in vacuo* and the residue was dissolved in 1 cm^3 of assay buffer (0·05 M sodium phosphate buffer, pH 7·4 containing 0·01 M EDTA, 0·2% gelatine, 0·1% Triton X-100 and 0·0001% Thiomerosal). The cardiac extracts were assayed for ANP using a rabbit anti-rat ANP serum (Peninsula Laboratories), cross-reactive with the equivalent human peptide and also cross-reactive with the hamster peptide and with negligible cross-reactivity to rat atriopeptin I, somatostatin, oxytocin or arg^8-vasopressin. Serial dilutions of the cardiac extracts, and rat ANP-28 (Peninsula Laboratories) as a reference standard, were incubated overnight at 4 °C with 50 μl of reconstituted ANP antiserum. Iodinated ANP (50 μl containing 10000 cpm; Amersham International) was added to the tubes and the samples were incubated for 24 hours at 4 °C. The separation of free and antibody-bound peptide was achieved by the addition of 50 μl sheep anti-rabbit Fc serum (generously provided by Professor P. J. Lowry, Reading University) diluted 1:20 and 50 μl non-immune rabbit serum (diluted 1:200). Following overnight incubation at 4 °C, 0·5 cm^3 assay buffer was added to the samples and they were centrifuged at 4000 rpm for 45 minutes at 4 °C. The supernatant was discarded and radioactivity in the precipitate was measured.

Recovery of ANP added to tissue extracts averaged 80% and the sensitivity of the assay was 1 fmol/tube. Coefficients of variation within and between assays were 5 and 6% respectively. The results were plotted against standards matched to a spline function fit.

Log transformation of the data was performed in order to reduce inequality of variance. Statistical significance was determined by analysis of variance and *post hoc* Duncan's multiple range test (SAS Inc).

RESULTS

Ultrastructural and immunocytochemical observations

Rat

The earliest stage of development at which membrane-bound electron-dense granules are detected in cardiac myocytes is after midday on the twelfth day of gestation (Fig. 1). At this stage, the heart is S-shaped but does not yet exhibit ventral looping. Myofibrils with recognisable Z-centres also make their first appearance about this stage although occasional groups of filaments, 6–10 nm thickness, can be recognised as scattered bundles 3–4 hours earlier on the same day. The earliest granules appear at the flanks of Golgi complexes near the nucleus and occasionally are sectioned in the process of budding from component cisterns; such early granules are small (100–300 nm in diameter) but possess the characteristic ultrastructural features of SHG, i.e. an electron-dense core separated by a narrow lucent interval from the

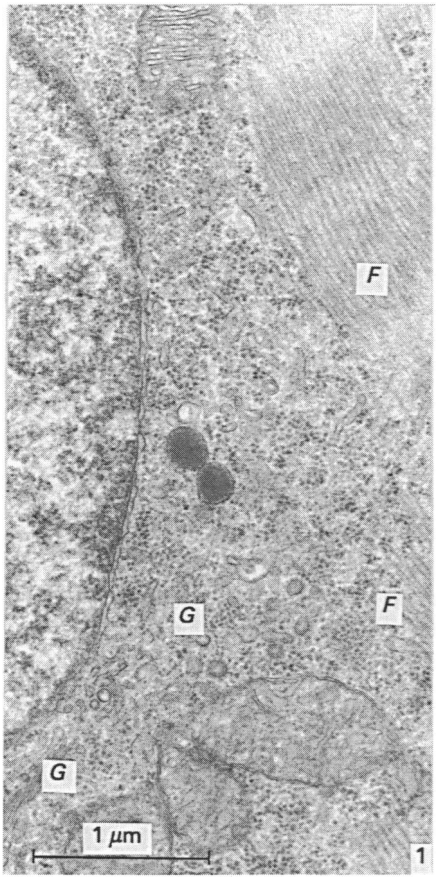
F
G
F
G
1 μm
1

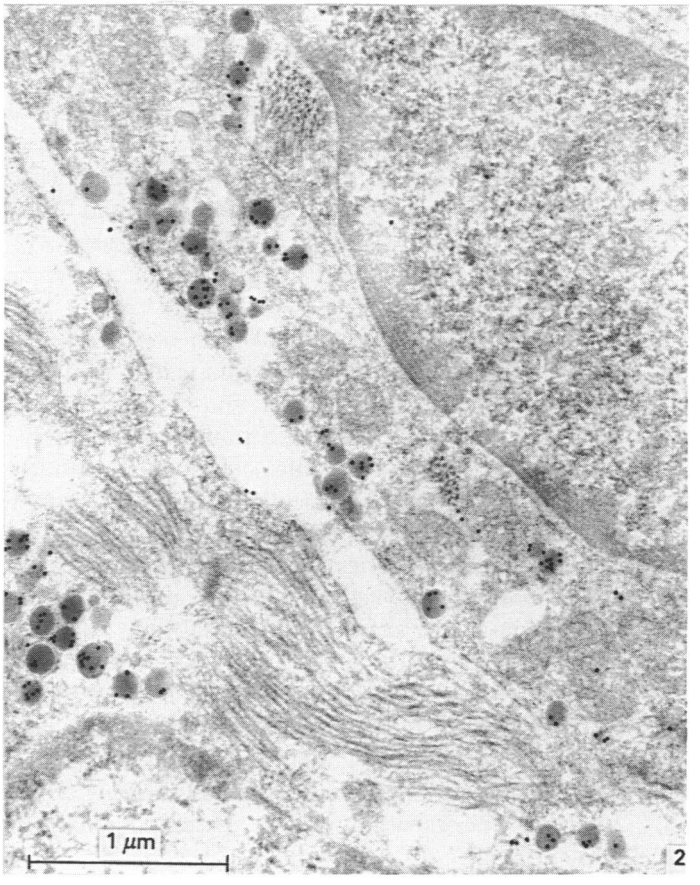
1 μm
2

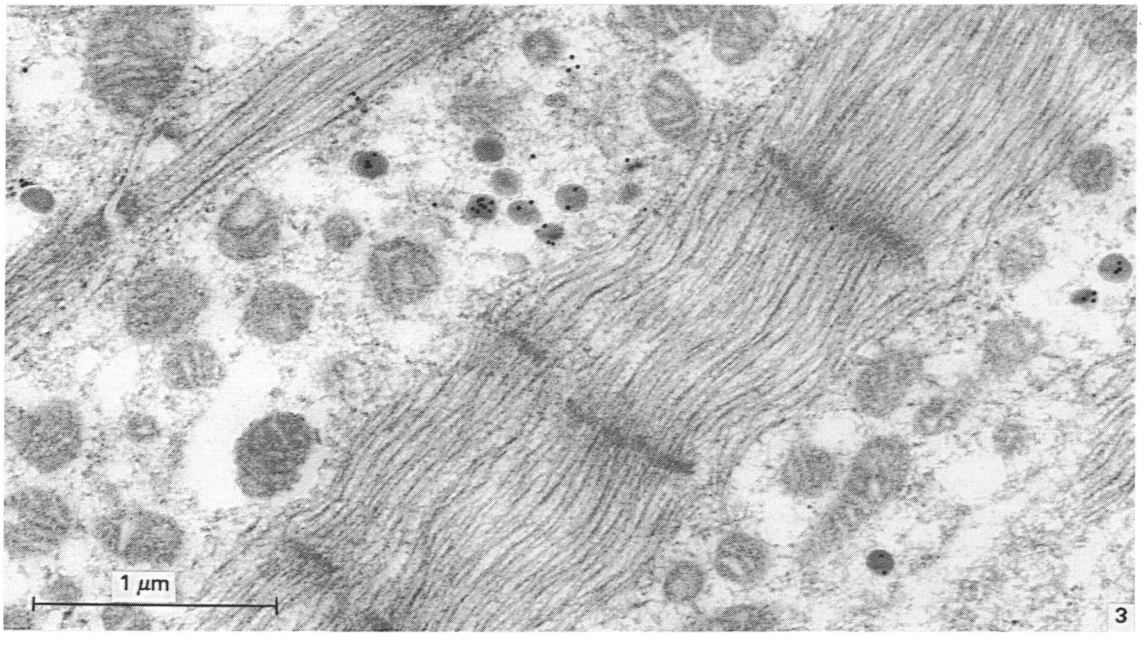
1 μm
3

limiting membrane, and the electron-dense material is immunoreactive for ANP-28. Cells containing immunoreactive SHG are scattered throughout the thickness of the myocardial sleeve of the cardiac rudiment and show no preferential distribution at this stage.

On Day 13, by which time looping is advanced in all planes and chamber formation has occurred, immunoreactive SHG are present in larger numbers (Fig. 2) and they can be identified in the myocardium of both atria and ventricles. They lie near cisterns of Golgi apparatus not only near the nucleus but also more peripherally, sometimes even near the sarcolemma. During subsequent fetal stages, cells expressing ANP are found in all regions of the atrial wall but myocytes adjacent to the endocardium or epicardium are more densely granulated than those in the main stratum between. In the adult, on the other hand, light microscopic inspection of immunolabelled sections after silver intensification shows that reactivity is relatively uniform and not localised to one or other surface layer. At no stage could differences in granularity or immunoreactivity be discerned between right and left atria.

As development proceeds, granules accumulate near the nuclear poles and along the sarcolemma of atrial myocytes. Generally, for the bulk of atrial myocytes, no specific intracellular polarity of granule accumulation was discernible in this study but, in older fetuses and in postnatal material, preferential clustering could be seen occasionally on the side of the cell adjacent to a capillary. A few granules are sufficiently superficial to bulge the sarcolemma, indicating possible sites of release, though clear exocytotic figures or pentalaminar figures indicative of membrane fusion are very rare in fetal myocytes. Multivesicular bodies are visible in atrial myocytes from the thirteenth day onwards and, though they are, in the main, negative for ANP-immunoreactivity, some of them contain small round deposits of electron-dense immunoreactive material resembling SHG.

SHG are established in ventricular muscle, as in atrial muscle, by 13 days of gestation (Fig. 3). Initially, the ultrastructural appearance of granules in the relevant ventricular cells closely resembles that in typical atrial cells; i.e. small immunoreactive SHG bud from cisterns of Golgi apparatus and spread from paranuclear regions to the periphery, including the subsarcolemmal region. However, granule-containing cells are sporadic within the ventricular wall and they vary considerably in granule content in contrast to the uniform granule content of atrial myocytes at the same stage of development; there is no evidence that ventricular myocytes containing immunoreactive SHG differ in any other ultrastructural feature, such as myofibrillar arrangement, from myocardial cells lacking granules nor is there evidence that the distribution of such cells corresponds with the distribution of the atrioventricular conducting system. The accumulation of granules in immunoreactive ventricular cells is similar to that in atrial myocytes until birth but, in neonatal hearts, granules decline in number so that only a few SHG are retained in any single ventricular myocyte (Fig. 4) in the vicinity of paranuclear Golgi complexes. Even though such cells are infrequent and scattered, careful search revealed them in all neonatal and adult hearts

Fig. 1. Electron micrograph of cell in myocardial sleeve of a 12 day rat fetus, showing two early specific granules, with limiting membrane and typical dense core, at the flanks of Golgi cisterns (*G*) in the perinuclear cytoplasm. Note the presence of formed myofibrillae (*F*) with Z disc material.

Fig. 2. LR white-embedded section through atrial myocardium of a 13 day rat fetus immunocytochemically labelled for ANP-28. The number of specific granules has increased considerably and some of them now lie near the sarcolemma.

Fig. 3. LR white-embedded section through ventricular myocardium of a 13 day rat fetus labelled for ANP-28. There are several labelled specific granules in the cytoplasm between myofibrillae.

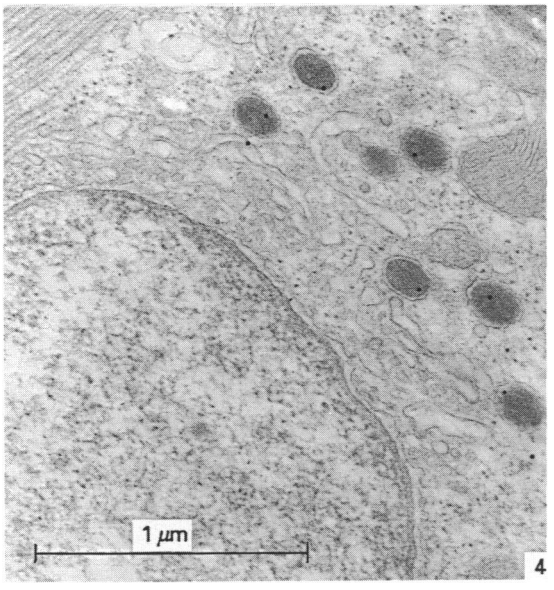
1 μm
4

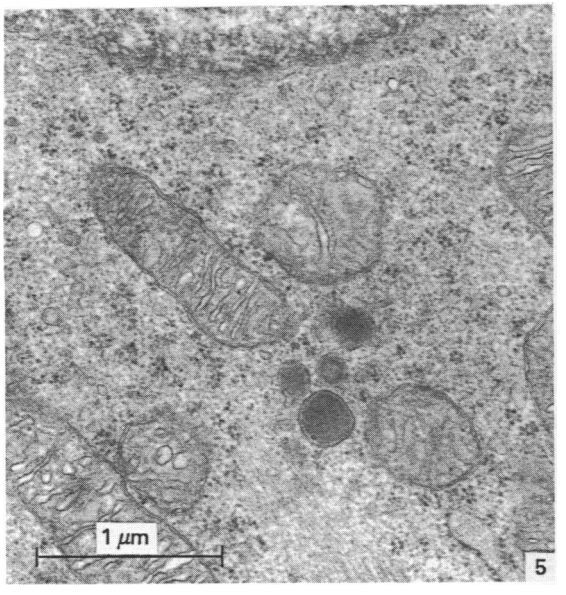
1 μm
5

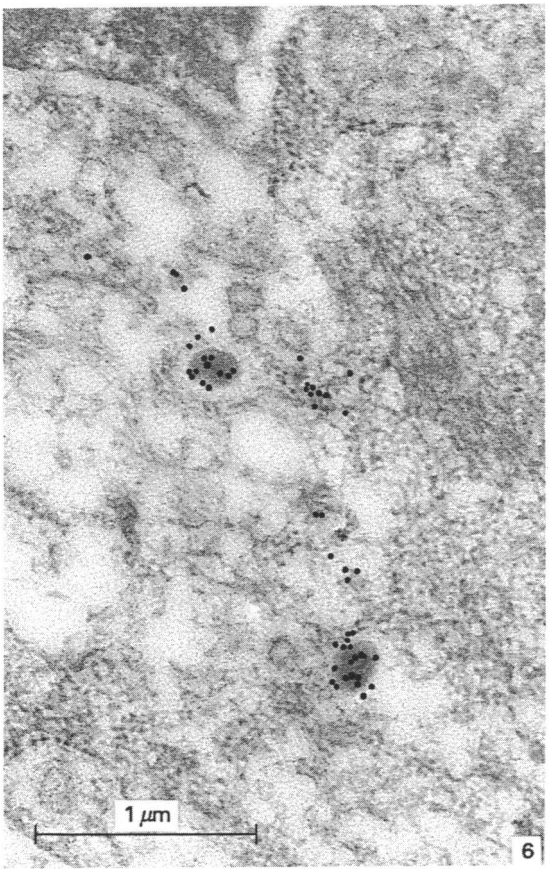
1 μm
6

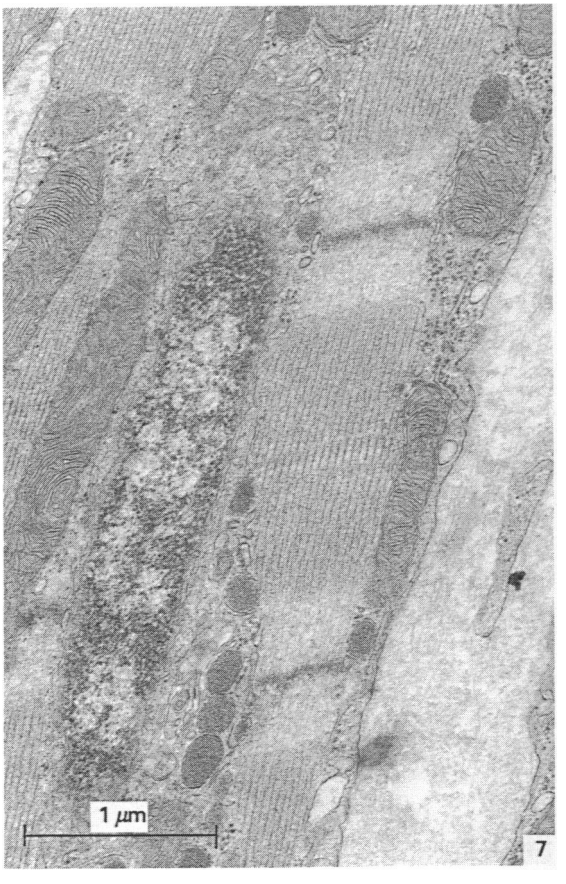
1 μm
7

that were examined. In postnatal ventricular cells, the Golgi apparatus itself shows altered morphology, being fragmented and more vacuolar than in corresponding atrial cells where it is more laminar or cisternal in structure.

Hamster

SHG appear in the hamster fetal heart on Day 10, at which stage the cardiac tube has begun but not completed the looping process preparatory to chamber formation (Fig. 5). The antiserum to alpha human-ANP which was used in this study is cross-reactive to the peptide in hamster SHG and the density of gold particles over granules in the hamster heart is similar to that in the rat.

The granules are immunoreactive from their first appearance (Fig. 6) and the pattern and sequence of SHG development in the hamster are similar to those in the rat though the granules are smaller and their population density is consistently lower. Within the atrium on Day 11, all cells seem to express such reactivity but in each cell profile the granules are more sparse than in rat fetuses at a corresponding stage of development (i.e. 12·5 days of gestation). The granules are found near the nucleus and also in peripheral cytoplasm; in atrial myocytes which lie subjacent to the endocardium or epicardium there is a tendency for the SHG to be polarised towards the free surface of sarcolemma. As in the rat, only a minority of ventricular myocytes contain immunoreactive SHG and these cells show no other special features either in ultrastructure or in position. SHG-containing cells are found throughout the atrial myocardium at all subsequent stages of development and there appears to be no difference in density of granularity between the two atria. The granularity of individual atrial myocytes increases during late fetal and neonatal stages (Fig. 7) in contrast to granule-containing ventricular myocytes which become even more sporadic in distribution and show no increase in granule density. At no stage is there an indication that the distribution of SHG-containing ventricular cells has any relationship to the distribution of the conducting system.

Radioimmunoassay

Rat

The results of ANP-radioimmunoassay of rat hearts are shown in Figure 8(*a*, *b*) and in Table 1. ANP-28 is first detected in pooled atria from 15 day fetuses (2·65 pmol mg^{-1} wet weight) and, subsequently, its level rises in both atria through the late fetal and neonatal stages. The difference in ANP-28 concentration between right and left atria is insignificant at all fetal stages, but two days after birth right atrial concentration exceeds that in the left ($P < 0{\cdot}05$) and this gradient tends to persist in postnatal life though not always at significant levels (Fig. 8*a*).

In the ventricles too the earliest detectable concentrations of ANP are found in 15 day fetal hearts (745 fmol mg^{-1}). Although they contain a significantly lower concentration ($P < 0{\cdot}05$), which is approximately one third of the concentration in

Fig. 4. Taab-embedded section through myocyte from the left ventricle of a 15 day neonatal rat labelled for ANP-28. Specific granules are fewer than before and they are restricted to the perinuclear region but they are characteristically labelled for ANP-28.

Fig. 5. Electron micrograph of section through myocardial sleeve in a 10 day hamster fetus showing early specific granules in the perinuclear cytoplasm.

Fig. 6. LR white-embedded section through myocardial sleeve of a 10 day hamster fetus immunocytochemically labelled for ANP-28. The specific granules are characteristically labelled for ANP-28 from the outset.

Fig. 7. Myocyte from right atrium of a 16 day hamster fetus showing numerous specific granules in the peripheral cytoplasm.

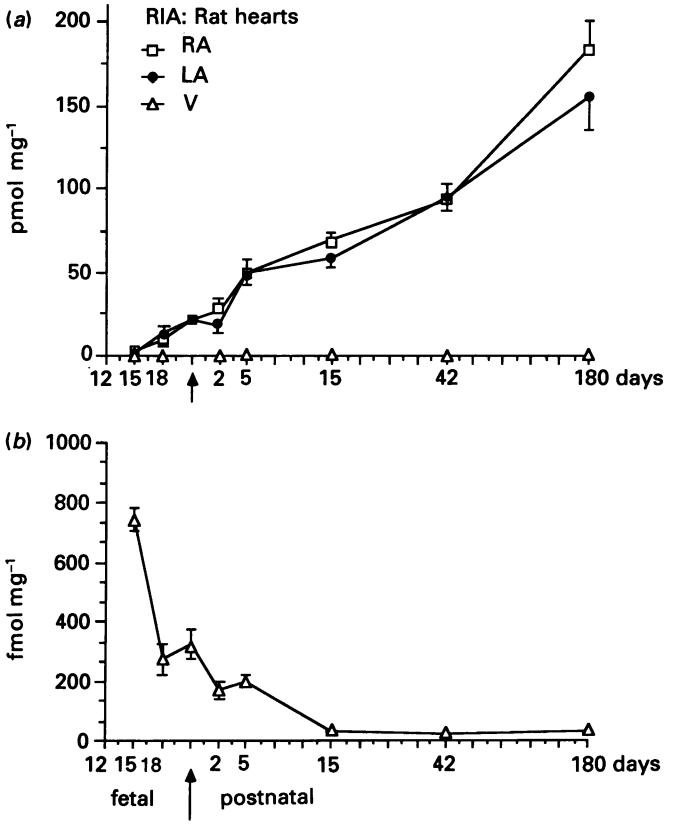

Fig. 8(*a–b*). Graph showing ANP concentrations as assessed by radioimmunoassay (RIA) in rat heart material. (*a*) Concentrations in the right atrium, left atrium and ventricles are compared. These concentrations become perceptible on the fifteenth day of gestation and atrial concentrations increase during subsequent fetal and neonatal periods. Right atrial concentrations of ANP exceed those in the left atrium in the early neonatal period and tend to maintain this gradient though not always at significant levels. (*b*) Shows ventricular concentrations on an expanded scale. The concentrations decrease during the late fetal and early neonatal periods to very low values.

Table 1. *Radioimmunoassay for ANP in rat hearts*

	Concentration (pmol mg^{-1} wet tissue ± SE)			Total content (pmol ± SE)	
Day	Right atrium	Left atrium	Ventricles combined	Atria combined	Ventricles combined
Fetus					
15	2·87 ± 1·0	2·43 ± 1·1	0·745 ± 0·037	2·60 ± 001·0	8·94 ± 0·04
18	10·43 ± 1·8	12·90 ± 2·8	0·273 ± 0·051	69·99 ± 013·8	5·19 ± 0·97
20	22·30 ± 2·0	22·20 ± 1·6	0·325 ± 0·053	178·00 ± 014·4	9·75 ± 1·59
Postnatal					
2	27·3 ± 02·5	18·50 ± 2·6	0·172 ± 0·031	256·30 ± 066·0	12·90 ± 2·33
5	50·4 ± 07·5	50·10 ± 4·7	0·197 ± 0·019	1005·00 ± 122·0	25·60 ± 2·47
15	58·8 ± 05·1	70·90 ± 6·0	0·029 ± 0·004	1615·20 ± 138·0	5·22 ± 0·72
42	93·2 ± 08·5	95·50 ± 8·3	0·020 ± 0·002	—	—
180	185·0 ± 16·0	156·00 ± 19	0·029 ± 0·002	—	—

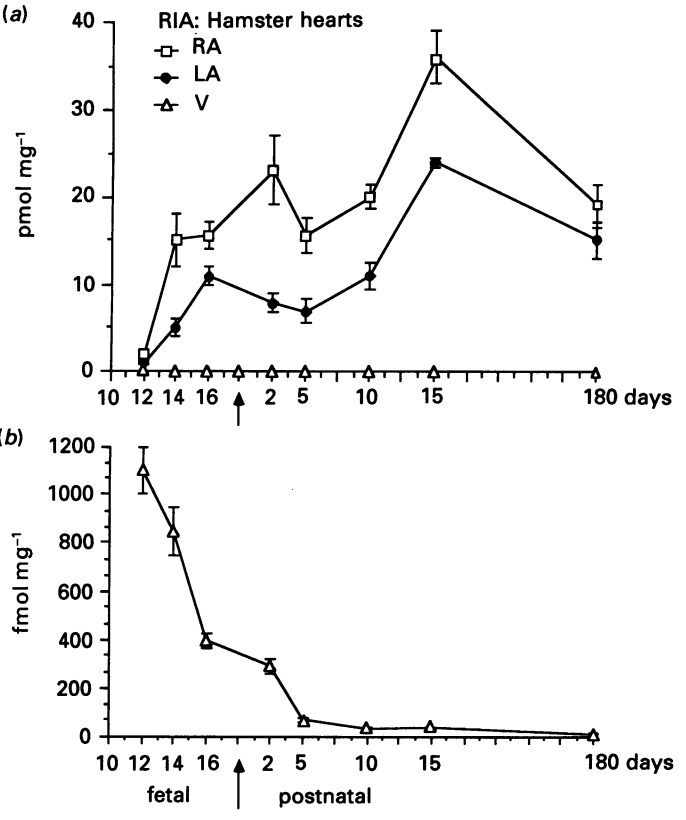

Fig. 9(*a–b*). Graph showing ANP concentrations as assessed by radioimmunoassay (RIA) in hamster hearts. (*a*) Concentrations of ANP in the right atrium, left atrium and ventricles are compared. These concentrations all become perceptible on the twelfth day of fetal life. Atrial concentrations increase during subsequent fetal and neonatal stages. Right atrial concentration exceeds left atrial concentration even during fetal stages. The gradient becomes exaggerated in the early neonatal period but narrows again in the adult. (*b*) Shows ventricular concentrations on an expanded scale and reveals that the ventricular level falls considerably during the late fetal and neonatal stages.

atrial tissue at the same stage (Fig. 8*a*), the total content in the ventricular myocardium at this time temporarily exceeds that in the atria (Table 1). The concentration in ventricular myocardium falls off to about 325 fmol mg^{-1} in 20 day fetuses and to 29 fmol mg^{-1} in 15 day neonates (Fig. 8*b*), a level which is maintained into adult life when atrial concentration exceeds it by a factor of 3×10^3. With decline in concentration, the total content of ANP-28 in the ventricles falls below that in the atria by the 18th day of gestation and, despite oscillations reflecting increased ventricular bulk with growth, ventricular content remains very low in comparison with atrial content (Table 1).

Hamster

The levels of ANP-immunoreactivity in the hamster heart, assessed by radioimmunoassay, are shown in Figure 9(*a*, *b*) and in Table 2. They become measurable in both atria and ventricles at 12 days of gestation and the concentrations are lower than in the rat at the corresponding initial stage and at all subsequent stages ($P < 0{\cdot}01$). The concentration in the right atrial wall exceeds that in the left ($P < 0{\cdot}01$) even before birth and the disparity peaks in the early neonatal period (Fig. 9*a*).

Table 2. *Radioimmunoassay for ANP in hamster hearts*

Day	Concentration (pmol mg^{-1} wet tissue ± SE)			Total content (pmol ± SE)	
	Right atrium	Left atrium	Ventricles combined	Atria combined	Ventricles combined
Fetus					
12	2·23 ± 0·4	1·24 ± 0·2	1·100 ± 0·1	1·32 ± 00·23	5·50 ± 0·40
14	15·20 ± 2·9	5·30 ± 1·0	0·850 ± 0·1	13·60 ± 02·57	3·40 ± 0·40
16	15·60 ± 1·6	10·90 ± 0·8	0·400 ± 0·03	45·20 ± 04·10	6·32 ± 0·46
Postnatal					
2	23·20 ± 4·0	7·70 ± 0·9	0·291 ± 0·033	137·20 ± 19·10	5·80 ± 0·70
5	15·60 ± 1·8	6·80 ± 1·5	0·071 ± 0·011	124·30 ± 16·90	4·40 ± 0·70
10	19·90 ± 1·7	11·20 ± 1·5	0·027 ± 0·005	195·90 ± 19·80	3·60 ± 0·70
15	35·70 ± 3·0	23·60 ± 0·7	0·035 ± 0·004	474·40 ± 32·00	5·40 ± 0·60
180	18·80 ± 2·7	15·50 ± 2·0	0·009 ± 0·004	—	—

The concentration of ANP in the ventricle is not significantly different from that in the atria at the outset (i.e. at 12 days of gestation) but, thereafter, the concentration falls (Fig. 9*b*); in the adult, atrial concentration exceeds it by a factor of about $1·5 \times 10^3$ ($P < 0·001$). Allowing for the greater bulk of the ventricular muscle mass, the total content of ANP in the ventricles is initially greater than that in the atria (Table 2) but, as in the rat, it declines to levels far below atrial content.

DISCUSSION

In this study, a similar sequence in the ontogeny of specific heart granules and related ANP activity could be discerned in the rat and the hamster. Immunoreactive specific heart granules first appear in cells of the myocardial sleeve on the twelfth day of gestation in the rat and on the tenth day of gestation in the hamster. At these dates the heart tube is at a similar developmental phase in both species, having commenced but not completed the looping processes which precede definitive chamber formation. The initial immunoreactive granules are closely associated with distended Golgi profiles and their first appearance is roughly concurrent with that of myofibrils. Most myocardial cells at this stage contain both specific granules and myofibrils suggesting that the expression of the relevant cardiac specific genes may be temporally related during differentiation.

Synthesis of ANP builds up after its initial appearance to become measurable by radioimmunoassay on the fifteenth day in the rat and by the twelfth day in the hamster by which time the heart is recognisably four-chambered in both species. At this stage, the measured concentrations of ANP immunoreactivity are lower in ventricular myocardium than in atrial myocardium but, in terms of content per chamber, ventricular ANP immunoreactivity exceeds that of atria.

In both species, the concentration of ANP immunoreactivity in the ventricles decreases after birth to trace levels in the adult (29 fmol mg^{-1} in the rat, 9 fmol mg^{-1} in the hamster). At fetal stages the genesis of SHG in ventricular cells is indistinguishable from that in atrial myocytes but, after birth, the Golgi profiles in ventricular myocytes are seen to vacuolate and fragment and the SHG are smaller in size and fewer in number; the ability to synthesise ANP is manifestly reduced even in those cells that retain it. It is possible that the induction of potential for ANP

expression occurs early in the differentiation of various cardiocytes and that the few ventricular cells that are capable of ANP synthesis were exposed to the relevant induction before terminal differentiation. In this study we could find no evidence for the view that SHG-containing cells in the ventricle are restricted to the conducting system as suggested by Toshimori, Toshimori, Oura & Matsuo (1987*a*, *b*) on the basis of their studies on rat and pig hearts. On the contrary, we have observed cells with immunoreactive SHG scattered sporadically throughout the working ventricular myocardium.

Within the fetal atria, almost all cells seem capable of ANP synthesis and the concentration of ANP immunoreactivity increases sharply with development even after birth. Recent light microscopic immunohistochemical investigations have suggested that ANP immunoreactivity is initially denser on the endocardial side of the myocardial layer and then shifts during development to the epicardial side (Scott & Jennes, 1987; Toshimori *et al.* 1987*a*); moreover, Cantin *et al.* (1984) reported depletion of granularity in the subendocardial layers of myocardium after birth, which they interpreted as stretch-mediated release of ANP. In this study, we could not find electron microscopic evidence for such shifts in distribution. At initial stages of granule development, the entire thickness of atrial myocardium does contain granules though they are most numerous in cells at the epicardial and endocardial aspects. During later development, there is no differential distribution of granule density. Nevertheless, some cells do exhibit an intracellular polarity in that granules tend to cluster at the surface nearest intramural capillaries or atrial endocardium.

In the adult rat, marked ultrastructural differences in granularity between the atria have been reported by Marie, Guillemot & Hatt (1976) and Cantin *et al.* (1984) but our qualitative ultrastructural studies did not reveal such a difference in fetal or neonatal material. Radioimmunoassay results in fetal rats indicate no significant difference in either the concentration or total content of ANP immunoreactivity between the right and left atria but a slight right to left gradient appears early in the postnatal period. In the hamster, on the other hand, right atrial levels exceed those on the left even on the twelfth day of gestation when ANP immunoreactivity first becomes measurable by radioimmunoassay. Higher levels in the right atrium are maintained till birth and, indeed, the difference becomes exaggerated in the 2- to 5-day period after birth and, thereafter, the gap narrows from the tenth day onwards. The exaggeration of the right to left gradient in the neonatal period may be caused by the increased stretch-mediated release of ANP, associated with the higher pressure in the left atrium. However, it is difficult to offer any explanation for the difference between the two atria in the prenatal hamster.

The ultrastructural observations on fetal material reported in the present study confirm the existing view that SHG are formed by budding from the Golgi apparatus, in paranuclear and peripheral positions, and that electron-dense material, which is immunoreactive for ANP, is synthesised intraluminally at these sites. In the absence of adequate plasma samples from young fetuses at the early stages of cardiogenesis, it is difficult to judge when ANP release from cardiac myocytes begins but the accumulation of granules immediately subjacent to the sarcolemma suggests that release may occur from about the thirteenth day of gestation in the rat and from the twelfth day in the hamster. The presence of multivesicular bodies containing ANP-immunoreactive granule material in 13 day rat fetal cardiocytes indicates that crinophagy of specific granules occurs from a very early stage of development.

SUMMARY

The ontogenesis of specific heart granules and of the related natriuretic peptide activity in heart muscle was studied in fetal and neonatal rats and golden hamsters by ultrastructural analysis including immunogold labelling for ANP-28 and by radioimmunoassay. In both species, immunoreactive granules first appear in the myocardial sleeve of the embryonic heart tube during the looping stages which precede chamber formation and the peptide becomes detectable by radioimmunoassay two or three days later by which time the chambers are identifiable. Granule density and ANP concentration in the rat are higher than in the hamster at all stages of development. Almost all atrial myocytes express ANP in fetal hearts whereas, in the ventricular wall, cells containing immunoreactive granules are scattered. The density of granules in atrial myocytes increases during further stages of fetal and neonatal development, while it decreases markedly even in those ventricular myocytes which are immunoreactive. Changes in the ultrastructural appearance of ventricular SHG suggest that the mode of production of ANP changes in ventricular myocytes after birth but does not change in atrial cells. There is no correlation between the distribution of immunoreactive ventricular myocytes and that of the conducting system. In both species, the concentration of ANP in the atrial well is higher than ventricular levels from the outset and the disparity becomes exaggerated with development till, in six months old adult animals, the atrial to ventricular concentration ratio is about 3×10^3:1 in the rat and $1{\cdot}5 \times 10^3$:1 in the hamster. In the hamster, a distinct gradient of ANP concentration between the right and left atria is already established in the early fetal period and it becomes enhanced in the neonatal period. In the rat, however, a slight difference becomes discernible only after birth.

The authors are indebted to Dr Nick Martensz for valuable guidance on radioimmunoassay technique and to Mr Bert Williams for technical assistance. They are also very grateful for grants from the Nuffield Foundation and from the Durham Fund, King's College, Cambridge.

REFERENCES

BENCOSME, S. A. & BERGER, J. M. (1971). Specific granules in mammalian and non-mammalian vertebrate cardiocytes. *Methods and Achievements in Experimental Pathology* **5**, 173–213.

CANTIN, M. & GENEST, J. (1985). The heart and the atrial natriuretic factor. *Endocrinology Reviews* **6**, 107–127.

CANTIN, M., GUTKOWSKA, G., THIBAULT, G., MILNE, R. W., LEDOUX, S., MINLI, S., CHAPEAU, C., GARCIA, R., HAMET, P. & GENEST, J. (1984). Immunocytochemical localisation of atrial natriuretic factor in the heart and salivary glands. *Histochemistry* **80**, 113–127.

CHALLICE, C. E. & VIRÁGH, S. (1973). The embryologic development of the mammalian heart. In *Ultrastructure of the Mammalian Heart* (ed. C. E. Challice & S. Virágh), ch. 3, pp. 91–126. New York: Academic Press.

CURRIE, M. G., GELLER, D. M., COLE, B. R., SIEGAL, N. R., FOK, K. F., ADAMS, A. P., EUBANKS, S. R., GALLUPPI, G. R. & NEEDLEMAN, P. (1984). Purification and sequence analysis of bioactive atrial peptides. *Science* **223**, 67–69.

DANSCHER, G. & RYTTER NÖRGAARD, J. O. (1985). Ultrastructural autometallography: a method for silver amplification of catalytic metals. *Journal of Histochemistry and Cytochemistry* **33**, 706–710.

DEBOLD, A. J., BORENSTEIN, H. B., VERESS, A. T. & SONNENBERG, H. (1981). A rapid and potent natriuretic response to intravenous injection of atrial myocardial extract in rats. *Life Science* **28**, 89–94.

DOLAN, L. M. & DOBROSZI, D. J. (1986). Atrial natriuretic factor (ANF) in the foetal rat: ontogeny and characterisation. *Journal of Cardiovascular Pharmacology* **8**, 1329.

MARIE, J.-P., GUILLEMOT, H. & HATT, P.-Y. (1976). Le degré de granulation des cardiocytes auriculaire. *Pathologie et Biologie* **24**, 549–554.

NAVARATNAM, V. (1987). *Heart Muscle: Ultrastructural Studies*. Cambridge University Press.

PAGER, J. (1968). Évolution structurale du tissu cardiaque en développement chez le foetus du rat. Thèse du 3° cycle, Lyon. Cited by Challice & Virágh (1973).

SCOTT, J. N. & JENNES, L. (1987). Distribution of atrial natriuretic factor in fetal rat atria and ventricles. *Cell and Tissue Research* **248**, 479–481.

SKEPPER, J. N. & NAVARATNAM, V. (1988). Analysis of the apparent heterogeneity of specific heart granules in rat atrial myocytes: an ultrastructural study including immunocytochemistry. *Histochemical Journal* **20**, 1–10.

TOSHIMORI, H., TOSHIMORI, K., OURA, C. & MATSUO, H. (1987*a*). Immunocytochemical study of atrial natriuretic polypeptides in the embryonic, foetal and neonatal rat heart. *Cell and Tissue Research* **248**, 627–633.

TOSHIMORI, H., TOSHIMORI, K., OURA, C. & MATSUO, H. (1987*b*). Immunohistochemistry and immunocytochemistry of atrial natriuretic peptide in porcine heart. *Histochemistry* **86**, 595–601.

TULASSAY, T., RASCHER, W. & LANG, R. E. (1986). Elevated plasma atrial natriuretic peptide (ANP) in premature children with renal disease. *Journal of Cardiovascular Pharmacology* **8**, 1303.

YUNGE, L., BALLAK, J., BEUZERON, J., LACASSE, J. & CANTIN, M. (1980). Ultrastructural cytochemistry of atrial and ventricular cardiocytes of the bullfrog (*Rana catasbeiana*). Relationship of specific granules with renin-like activity of the myocardium. *Canadian Journal of Physiology and Pharmacology* **58**, 1463–1476.